Science of the Total Environment 574 (2017) 139–147

Contents lists available at ScienceDirect

Science of the Total Environment

journal homepage: www.elsevier.com/locate/scitotenv

The role of biochar porosity and surface functionality in augmenting hydrologic properties of a sandy soil

Waled Suliman [a], James B. Harsh [a], Nehal I. Abu-Lail [b], Ann-Marie Fortuna [c], Ian Dallmeyer [d], Manuel Garcia-PérezAssociate Professor [d,*]

[a] Department of Crop and Soil Sciences, Washington State University, Pullman, WA 99164, USA
[b] The Gene and Linda Voiland School of Chemical Engineering and Bioengineering, Washington State University, Pullman, WA 99164, USA
[c] Soil Science Department, North Dakota State University, Fargo, ND 58108, USA
[d] Composite Materials and Engineering Center, Washington State University, Pullman, WA 99164, USA

HIGHLIGHTS

- Oxidized biochars retain more water than unoxidized ones.
- Air oxidation of biochar is a suitable way to enhance water holding capacity of biochar and its blends with soils.
- There is a positive correlation between total acidic functional groups on the surface of biochar and soil water retention.
- The capability of biochar to retain soil water is a function of the combination of its porosity and surface functionality.

GRAPHICAL ABSTRACT

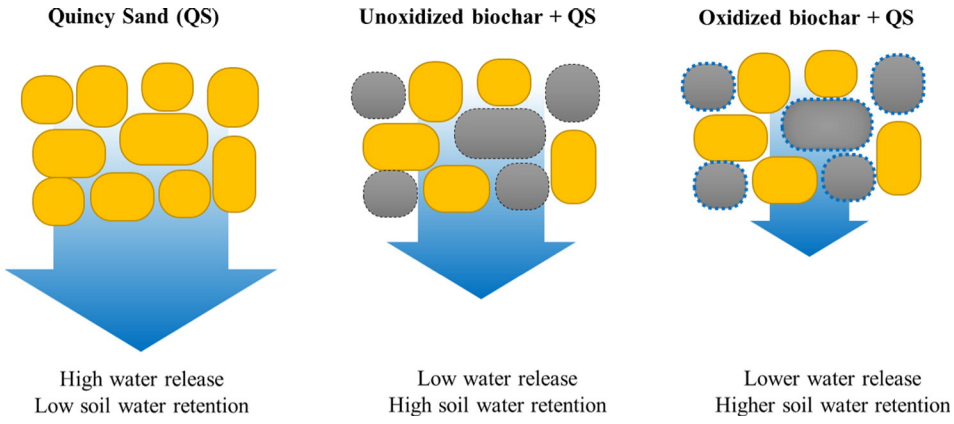

ARTICLE INFO

Article history:
Received 28 May 2016
Received in revised form 3 September 2016
Accepted 4 September 2016
Available online xxxx

Editor: Ajit Sarmah

Keywords:
Oxidized biochar
Soil water retention
Quincy sand
Hydrological properties of biochar

ABSTRACT

This paper reports studies to elucidate the potential relationships between porosity and surface functionality of biochar and soil water retention characteristics. The biochars studied were produced from pine wood (PW), hybrid poplar wood (HP), and pine bark (PB) at temperatures of 350 °C and 600 °C. The resulting materials were then oxidized under air at 250 °C to generate oxygenated functional groups on the surface. All biochar were thoroughly characterized (surface and bulk properties) and their hydrological properties measured in blends with Quincy sand. We prepared 39 microcosms for this study to examine the effect of biochar functionalities and porosity on the hydro-physical properties of Quincy sand. Each biochar was thoroughly mixed with the soil at 20 g kg^{-1}. The field capacity, wilting point, and total available soil moisture of the bio-char/Quincy sand mixtures were measured for both dry and wet ranges. The soil water potentials and soil water contents were fitted using the model of van Genuchten. Our results indicated that the amount of oxygenated functional groups on the surface of biochars clearly differentiated the biochars in terms of hydrophilicity, with the oxidized biochars being superior, followed by the low-temperature biochars, while the high temperature biochars possessed lowest hydrophilicity. As a result, oxidized biochars exhibited better wettability compared to unoxidized biochars,

* Corresponding author at: Biological Systems Engineering, WSU, LJ Smith, Room 205, Pullman, WA 99164-6120, USA.
E-mail address: mgarcia-perez@wsu.edu (M. Garcia-Pérez).

http://dx.doi.org/10.1016/j.scitotenv.2016.09.025
0048-9697/© 2016 Elsevier B.V. All rights reserved.

regardless their feedstock source. Significant correlation occurred between the total acidic functional groups on biochar surface and water contents at different matric potentials. Over a wide range of soil water potentials, oxidized biochar-soil mixtures held more water than the unoxidized biochar-soil mixtures except in the region between −0.1 and −5 kPa of ψ, which is near saturation. Soil water contents at different matric potentials were significantly inter-correlated ($P < 0.01$) and correlated with bulk densities of biochar-amended soil samples.
© 2016 Elsevier B.V. All rights reserved.

1. Introduction

Biochar application to soils is not a new concept; it was used successfully by generations of indigenous farmers in the Amazon basin (Maia et al., 2011). Accumulation of bulky quantities of biochar increased soil agronomic quality and formed what is known as Amazonian Dark Earths (or *Terra Preta*) which are still highly valued soils for agricultural and horticultural use (Verheijen et al., 2010). Biochar, as a term, is reserved for any carbon-enriched porous material that has been chemically and structurally altered through thermo-decomposition via anaerobic pyrolysis and that is used specifically as a soil amendment (Forbes et al., 2006; Lehmann et al., 2006). Properties of biochar depend on the original biomass (chemical composition, ash content, particle size), the production conditions (temperature, residence time, oxidative conditions), the pre-treatment procedures (drying, crushing), and the post-treatment processes (i.e. activation method) (Copeland et al., 2008; Lehmann and Joseph, 2009).

Use of biochar is a sustainable option to provide long-lasting improvements in soil fertility (Lehmann et al., 2003; J.M. Novak et al., 2009a), especially in sandy soils where sustainable agriculture faces large constraints due to low water holding capacity, and high leaching of soil nutrients (Uzoma et al., 2011). Because of its ability to retain nutrients and to improve soil water holding capacity, biochar soil application can be used to overcome some of the limitations faced when land farming sandy soils (i.e. additional requirements for artificial fertilizers and intensive irrigation) providing a promising soil management option for these conditions. Positive effects of biochar on soil properties and plant growth in sandy soil are well documented (Basso et al., 2013; Uzoma et al., 2011). Recent studies have shown that biochar soil additions increase pH of acidic, enhance cation exchange capacity (CEC), increase soil water-holding capacity, modify soil bulk density, and increase exchangeable basic cations soils (Basso et al., 2013; J. Novak et al., 2009b; Liang et al., 2006; Sika, 2012).

While greater scientific attention has resulted in an increasing number of biochar publications, there is still a need for further research with respect to how the biochar affects some of the limiting factors of agricultural production in sandy soils. Little work has been done to address the use of biochar application to enhance the hydrological properties of theses soils. In addition, there is a need for research that investigates the relationship between the surface chemistry of biochar and water hydrological characteristics of biochar amended soils. In particular, the effects of biochar porosity and surface functionalities' effects on the hydro-physical properties of a sandy soil are relatively unknown compared to other common parameters (e.g. application rate, pyrolysis temperature, feedstock source). Hence, the goal of this study is to evaluate the effect of biochar bulk and surface properties on hydro-physical properties of Quincy sand-biochar blends, as well as to explore the potential of oxidized biochar to retain water in the Quincy sand.

2. Material and methods

2.1. Biochar preparation

Biochars were produced at the biomass thermochemical conversion laboratory at Washington State University from Pine Wood, Pine Bark and Poplar Wood. The Lab scale spoon reactor, Fig. 1, was operated at two pyrolysis temperatures: 350 °C and 600 °C representative of the lower and upper pyrolysis thresholds for biochar formation. More details on the production methods are shown in Section 1 of the supplementary material. Here, biochars are denoted as PW for the pine wood feedstock and PW-350, and PW-600 for the resulting unoxidized biochars created at 350 and 600 °C, respectively. The oxidized samples are abbreviated as AO referring to air oxidation. Similar abbreviation procedure was applied for the pine bark (PB) and hybrid poplar wood (HP) batches.

2.2. Biochar characterization

The bulk and surface characterization of the biochars studied in this paper were reported elsewhere (Suliman et al., 2016a,b). A brief description is shown in the supplementary material (Section 2). Some of the most important properties of the 'biochar' tested that are relevant for this study are summarized in Table 1.

2.3. Soil

The Quincy sand (QS) was used in this study because it is present on nearly 285,000 ha in Washington, Oregon, and Idaho, and is an agriculturally important soil in the Pacific Northwest region of the US (http://www.nrcs.usda.gov/wps/portal/nrcs/soilsurvey/soils/survey/state/). The sand was collected, air-dried, and sieved through a 2 mm mesh. Some selected physical and chemical characteristics are shown in Table 2. To measure the soil zeta potential, 5 g of the soil was added to 100 ml of deionized water and agitated on an orbital shaker for 6 h at 25 °C. The aliquot of the supernatant was then collected (decanted from the container) and analyzed by Nano-Zetasizer 3000 (Malvern Instruments Ltd., Malvern, UK).

2.4. Experimental design

Thirty nine microcosms were prepared for this study to examine the effect of biochar on hydro-physical properties of Quincy sand. Each biochar was thoroughly mixed with the soil at a rate of 20 g biochar kg^{-1} soil. The mixing rate was calculated by assuming 15 cm and 1.5 g cm^{-3} for soil depth and bulk density, respectively. Three replicates of 30 g of each mixture were then packed into plastic containers. Bulk density, porosity, organic matter, pH, and EC were determined for biochar-soil mixtures using the methods described previously in Section 2.2 for the biochar. These mixtures were abbreviated as QS, QS-HP350-UO, QS-HP600-UO representing the soil control (Quincy sand alone), soil with unoxidized HP biochar produced at 350 °C (HP350), soil with unoxidized HP biochar produced at 600 °C, respectively. The same abbreviation were utilized for soil with unoxidized PW and PB biochars, and for oxidized samples but with adding AO.

2.5. Soil hydraulic measurements

To evaluate the influence of biochar on the water relations of sandy soil, consideration must be given to the effect on field capacity, wilting point and total available soil moisture. In the present study, soil water retention was measured on intact soil microcosms for both dry and wet ranges. A T5 Tensiometer (UMS GmbH, Munich, Germany) was used to measure metric potential above −100 kPa, whereas a WP4C

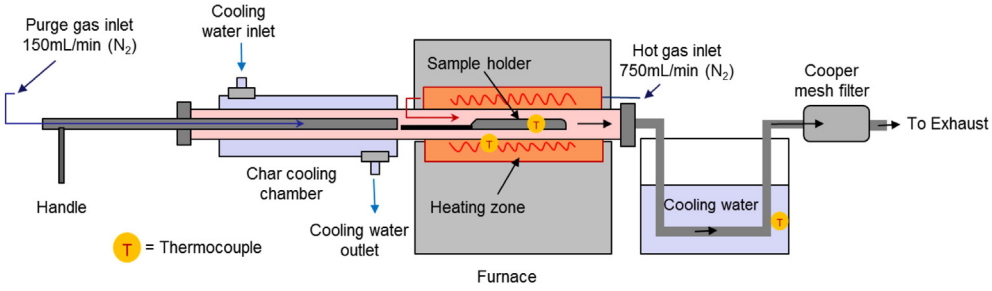

Fig. 1. A scheme of the lab-scale spoon pyrolysis reactor used in this study.

dew point potentiometer (Decagon Devices, Inc., Pullman, WA) was used to measure water potential below −100 kPa. For wet range, the soil microcosms were water-saturated from the base, and allowed to reach equilibrium, water potentials and water content were then measured. The effects of osmotic potential are generally considered negligible when only liquid water flow is considered; however, it is an important parameter for soil microbial processes (e.g. nitrification and ammonification) as well as plant root activity (Low et al., 1997). In this study, osmotic potential was calculated by multiplying EC (dS m^{-1}) by −36 (kPa). Volumetric water content was calculated as follows:

$$\theta = u\frac{\rho_b}{\rho_w} \quad (1)$$

where θ is the volumetric water content ($cm^3\ cm^{-3}$), u is the gravimetric water content ($g\ g^{-1}$), ρ_b is the soil bulk density ($g\ cm^{-3}$), and ρ_w is the density of water (assumed to be 1 $g\ cm^3$).

In order to determine permanent wilting point (θ_{PWP}), a simple indirect method of Decagon Devices Inc. was followed using the WP4C. Briefly, air-dried sandy soil samples were assumed to have 0.008 $g\ g^{-1}$ and 0.003 $g\ g^{-1}$ water contents at −1.5 MPa and air dry condition, respectively. To reach θ_{PWP}, a small amount of water was added to air-dried soil according to the following calculation:

$$M_w = M_{ad}\frac{w - w_{ad}}{1 - w_{ad}} \quad (2)$$

where M_w is mass of water to add (g), M_{ad} is the mass of air dried soil sample (g), w is the assumed sand water content at −1.5 MPa ($g\ g^{-1}$), and w_{ad} is the assumed mass of water for air dried sand samples ($g\ g^{-1}$). After equilibration, water potential was measured using WP4C, and water content was determined using the oven drying method. The gravimetric water content at −1.5 MPa was computed following the equation:

$$w_{-1.5} = w_m\frac{\ln\left(\frac{-1000}{-1.5}\right)}{\ln\left(\frac{-100}{\Psi_m}\right)} \quad (3)$$

where $w_{-1.5}$ is the gravimetric water content at −1.5 MPa ($g\ g^{-1}$), w_m is the measured mass water content ($g\ g^{-1}$), Ψ_m is the measured water potential (MPa). Finally, gravimetric water content was converted to volumetric water content by multiplying the gravimetric water content by the soil bulk density.

The water content at field capacity (θ_{FC}) is defined as the volume of water held at a water potential (Ψ) between −10 and −30 kPa, while water content at permanent wilting point (θ_{PWP}) is described as the moisture content in soils at which plants begin to wilt and cannot recover in a saturated atmosphere without increasing moisture in the soil. The water content at field capacity (θ_{FC}) was determined by an overnight free drainage method (de Melo Carvalho et al., 2014; Song and Guo, 2012): saturated samples were put in plastic containers with meshed bottom, covered by Para-film to prevent evaporation, and then left 24 h to drain. The moisture retained was taken as field capacity and measured using the oven-dry method. Available water content (AWC) and readily available water content (RAWC) were calculated by subtracting the volumetric water content at −1500 and −10 kPa, respectively, from the water content at field capacity (Quin et al., 2014). The available water content represents the quantity of water that can be held and would be available to the plant. The water release curves were obtained by plotting the volumetric water content against the matric potential following the method described elsewhere (Abel et al., 2013; Rossi and Nimmo, 1994; Stoof et al., 2010).

Table 1
General physico-chemical properties of biochars (Suliman et al., 2016a,b).

	PW-350		PW-600		PB-350		PB-600		HP-350		HP-600	
Property	UO	AO	UO	AO	UO	AO	UO	AO	UO	AO	UO	AO
C (wt.%)	70.50	65.37	87.80	85.08	66.07	63.85	78.11	78.07	69.91	65.43	83.07	81.41
O (wt.%)	23.15	29.17	7.06	10.27	23.67	27.11	8.98	10.21	20.86	24.94	6.84	8.78
Bulk density ($g\ cm^{-3}$)	0.14	0.14	0.24	0.24	0.61	0.61	0.21	0.21	0.13	0.13	0.13	0.13
Particle density ($g\ cm^{-3}$)	0.56	0.56	0.7	0.7	0.45	0.45	0.48	0.48	0.52	0.52	0.85	0.85
Porosity (%)	71	71	78	78	64	64	68	68	69	69	81	81
pH_{H2O}	8.20	7.8	8.79	8.10	7.88	7.5	10.19	9.00	10.00	9.1	10.41	9.3
pH_{pzc}	3.0	1.2	5.6	3.2	1.4	1	4.4	3.7	1.1	1.1	2.2	1.5
TOFGs (atom %)	45.59	49.95	16.79	29.64	57.31	75.54	9.22	23.46	43.57	50.04	13.09	23.81
TAFGs ($mmol\ g^{-1}$)	0.15	0.61	0.03	0.13	0.16	0.34	0.02	0.12	0.14	0.34	0.01	0.08
TBFGs ($mmol\ g^{-1}$)	0.01	0.00	0.03	0.02	0.04	0.03	0.11	0.11	0.06	0.05	0.13	0.10
SA ($m^2\ g^{-1}$)	146	190	500	570	172	187	424	550	208	171	417	557
TPV ($cm^3\ g^{-1}$)	0.14	0.23	0.57	0.75	0.20	0.24	0.43	0.81	0.27	0.20	0.65	0.87

Abbreviations: PW, PB and HP = pine wood, pine bark, and hybrid poplar wood biochars, 350 and 600 = pyrolysis temperature (°C), UO = un-oxidized biochar; AO = air-oxidized biochar, C = total carbon content (wt.%), O = Total Oxygen content (by difference), pH_{pzc} = the pH of zero point charge, TOFGs = total oxygen functional groups measured by XPS technique (atom %), TAFGs = total acidic functional groups ($mmol\ g^{-1}$), TBFGs = total basic functional groups ($mmol\ g^{-1}$), SA = surface area ($m^2\ g^{-1}$), and TPV = total pore volume ($cm^3\ g^{-1}$).

Table 2
Selected physicochemical properties of the Quincy sand.

Characteristic		Measurement
Bulk density (g cm^{-3})		1.49
Particle density (g cm^{-3})		2.62
Porosity (vol.%)		43.23
Moisture content (wt.%)		0.55
Water holding capacity (wt.%)		16.91
Organic matter (wt.%)		0.75
$pH_{(H2O)}$ [a]		7.5
$EC_{(H2O)}$ (ds m^{-1})[a]		0.08
CEC (C-mol_c kg^{-1})		3.5
NH_4^+ (mg N kg^{-1})		0.035
NO_3^- (mg N kg^{-1})		1.583
Zeta potential at pH 7		−23
Particle size (texture)	Sand (wt.%)	95.1
	Silt (wt.%)	3.4
	Clay (wt.%)	1.5

[a] The pH and EC were measured in a 1:5 (mass/vol) dry-soil: de-ionized water.

2.6. Retention modeling and data evaluation

The soil water potentials and soil water contents were fitted using the model of van Genuchten (1980), which was selected based on the conspicuous higher degree of fitting and the unimodal behavior of our data. To obtain the soil water retention curve of van Genuchten model, the SWRC-Fit version 1.3 software (Seki, 2007) was used; it can also be executed directly from the web page (http://purl.org/net/swrc). The van Genuchten function with the Mualem restriction ($m = 1–1/n$) (van Genuchten, 1980; Mualem, 1986) is given by:

$$\theta(\psi) = \theta_r + (\theta_s - \theta_r) \cdot \left[\frac{1}{1 + (\alpha|\psi)^n}\right]^m \quad (4)$$

where $\theta(\psi)$ is the volumetric water content [cm^3 cm^{-3}] at given matric potential ψ (kPa), θ_s is the saturated water content [cm^3 cm^{-3}] when $\psi = 0$ kPa, θ_r is the residual water content [cm^3 cm^{-3}] at $\psi \geq -1500$ kPa, and α, n, and m are shape parameters. The Mualem constraint ($m = 1 - 1/n$) was adopted to increase model parsimony (de Melo Carvalho et al., 2014).

A completely randomized design was used for this study; 12 treatments were randomly assigned to soil containers within the same constant-temperature room. The main goal of this analysis was to compare the effect of two biochar production factors on the measured soil hydro-physical properties. A two-way analysis of variance was used to determine significance of the biochar produced from 3 parent feedstocks and under 2 pyrolysis temperatures. All statistical analyses were conducted using Minitab (version 17, Minitab, Inc., State College, PA).

3. Results and discussion

3.1. Hydro-physical properties of biochar

The biochars used were comprehensively characterized both in their raw forms and after oxidation by air at 250 °C. Biochar particle size distribution, porosity, surface functionality and hydrophobicity are discussed below. Other selected results are summarized in Table 1 and a more comprehensive data set is available in our previous publications (Suliman et al., 2016a,b).

3.1.1. Particle size distribution

Fig. 2 shows the particle size distribution for the sand investigated as well as biochars used in this study. The sand has an approximately Gaussian distribution centered near 229 μm with particles generally constricted to 10–500 μm. Biochars, except the PB-350, are somewhat larger, with mean particle sizes near 300–470 μm. These samples also show a strong asymmetric distribution towards lower particle sizes, i.e. PB-600. The distribution occurs over a range of 10–175 μm for all biochars. (See Fig. 3.)

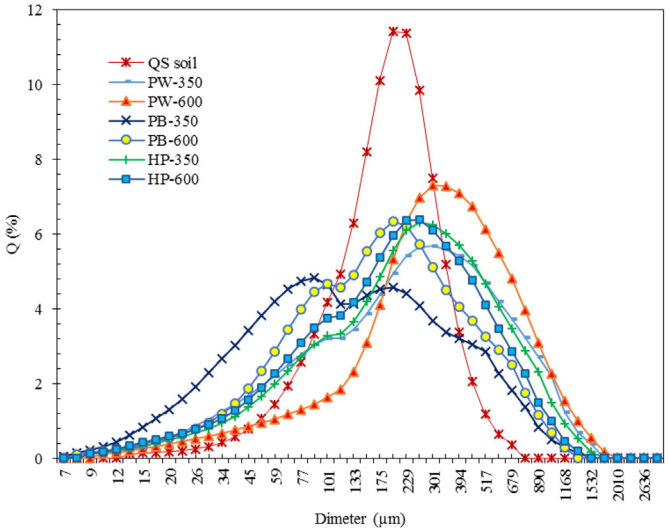

Fig. 2. Particle size distribution of soil and biochars.

3.1.2. Porosity and functionality of biochar

The difference in the pyrolysis temperature and air oxidation of biochar resulted in significant changes in the internal porosity and surface functionality (Suliman et al., 2016a,b). A side-by-side comparison of low- and high-temperature biochars shows that microporous structure and surface chemistry both altered significantly when pyrolysis temperature reached its highest degrees (Table 3). At 600 °C, the surface area and pore volume increased considerably compared to those of biochars produced at 350 °C. This result was likely due the formation of micropores on the biochar surface. Our results also showed that the surface area of biochars produced at high temperature (i.e. 600 °C) increased significantly after being oxidized by air at 250 °C; micropore surface area increased from 500 to 570, 424 to 550, and 417 to 557 m^2 g^{-1} in PW, PB, and HP biochars, respectively. The increase in area can be explained by the removal of some walls of the carbonaceous material during oxidation as proven by the correlation between burn-off degree and micropore volume, details can be found in our previous publication

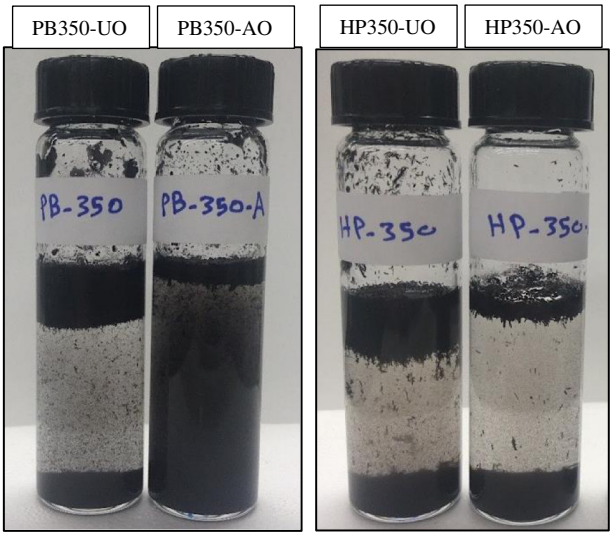

Fig. 3. Wettability/dispensability behavior of PB-350 and HP-350, unoxidized (UO) and oxidized (AO) biochars. The content in each of the bottles was 0.5 mg/15 ml and they were sonicated for 10 min.

Table 3
Characteristics of microporous structure of unoxidized (UO) and oxidized (AO) PW, PB, and HP biochars as a function of pyrolysis temperature.

Sample ID	PV_{mic}[a] ($cm^3\ g^{-1}$)		PV_{tot}[b] ($cm^3\ g^{-1}$)		SA_{CO2}[c] ($m^2\ g^{-1}$)		Pore size distribution of oxidized biochar (%)			
	UO	AO	UO	AO	UO	AO	<0.5 (nm)	0.5–0.7 (nm)	0.7–0.9 (nm)	>0.9 (nm)
PW-350	0.06	0.08	0.14	0.23	146	190	1.80	26.06	35.25	36.9
PW-600	0.20	0.23	0.57	0.75	500	570	2.02	25.98	35.00	37.00
PB-350	0.07	0.07	0.20	0.24	172	187	2.29	26.58	35.04	36.09
PB-600	0.17	0.22	0.43	0.81	424	550	2.50	26.8	36.28	37.62
HP-350	0.08	0.07	0.27	0.20	208	171	2.02	26.26	35.34	36.38
HP-600	0.17	0.22	0.65	0.87	417	557	2.65	26.8	37.43	38.57

[a] Micropore volume.
[b] Total pore volume.
[c] Surface area calculated from fitting of the DR equation.

(Suliman et al., 2016b). The SEM analysis, presented in (Suliman et al., 2016a), did not show any significant effects of air oxidation on surface roughness or cavity size in micro-ranges, implying that the oxidation effect may have occurred at only the nano-range scale. In terms of large pores (>0.5 μm), all biochars used in this study contained cavities between 0.5 and 300 μm in diameter which would have an important role the quantities of water help.

The surface composition determined by XPS and Boehm titration showed that the amount of oxygen-containing functional groups in unoxidized samples decreased as the pyrolysis temperature increased. This result is mainly due to the removal of oxygenated functional groups from the surface of biochar as the carbonization temperature increased from 350 to 600 °C. However, after oxidation by air, oxygen functional groups were formed on the surface of the biochar samples, and thus oxidized biochars had higher surface oxygen fractions. Furthermore, the formation of surface oxygen functional groups, i.e. carbonyl and carboxyl groups, contribute additional negative charges to the surface and consequently the pH at the point of zero charge is always higher for unoxidized bio-chars. Moreover, our results suggest that the distribution of oxygen was obviously heterogeneous and the oxygen functional groups were primarily fixed on the more external surface of the samples, as confirmed by comparing XPS results with those of elemental analysis, more details can be found in our previous publication (Suliman et al., 2016b).

3.1.3. Hydrophobicity and wettability

Table 4 shows the hydrophobicity index and water drop penetration time (WDPT) of biochar used in this study. In agreement with Gray et al. (2014) and Kinney et al. (2012) who reported that high pyrolysis temperature leads to less hydrophobic biochar surfaces. Our results showed that biochar hydrophobicity decreased as pyrolysis temperature increased, as indicated by MED index but not by the WDPT technique.

Table 4
Hydrophobicity index and water drop penetration time (WDPT) of biochar.

Biochar		Hydrophobicity (MED index)	WDPT (s)
QS-PW-350	UO	0.7	50
	AO	0.0	0
QS-PW-600	UO	0.2	2
	AO	0.0	1
QS-PB-350	UO	30.0	>60
	AO	10.0	>60
QS-PB-600	UO	1.0	>60
	AO	0.3	10
QS-HP-350	UO	10.0	>60
	AO	2.5	>60
QS-HP-600	UO	0.9	>60
	AO	0.0	2

Biochar hydrophobicity varied from extremely hydrophobic (MED = 30 for PB-350) to hydrophilic (MED = 0.1 for PW-600). This particular observation could be explained by the changes in surface chemistry as a function of temperature (Suliman et al., 2016a). Das and Sarmah (2015) suggested that the hydrophobicity of a biochar made at low pyrolysis temperature is not permanent due to the displament of tar like compounds when subjected to water. Across all feedstocks we observed that PB-350 and HP-350 were both extremely hydrophobic compared to their countrpart (i.e. PW-350), implying feedstock-related chemical and physical differnces. The oxidized biochars (i.e. PW-350-AO, PW-600-AO, and HP-600-AO) were extremely hydrophilic (MED = 0) compared to their unoxidized countrparts (MED = 0.7, 0.2, and 0.9, repectively). The availability of oxygen-containing groups for water binding was determined by the polarity and hydrophobicity indexes of biochar surfaces. The polarity indexes [(O + N)/C] of our biochars (Suliman et al., 2016a) indicated that oxidized biochars exhibit higher index values and therefore low hydrophobicities compared to their unoxidized counterparts. According to Bradley et al., 2011 and Kinney et al., 2012, the availabiltiy of polar groups, such as C—O/C═O, on biochar surfaces usually act as water-binding centers and assist the formation of water clusters. Therefore, these surfaces should be covered with a thin layer of water in aqueous solutions. Moreover, as seen in Fig. 4, oxidized biochars exhibited better wettability in comparison with unoxidized biochars, and were more dispersible even after 10 min of sonication. The low sedimentation rates of unoxidized biochars indicate lower wettability and higher hydrophobic character.

3.2. Characteristics of soil water retention curves (SWRC)

The change in the soil-water retention characteristics after biochar additions is shown in Fig. 5. Untreated Quincy sand (control) retained a relatively smaller amount of water, even at high soil water potentials. We observed that addition of biochar increased soil water retention in both high and low potential ranges compared to the control. Two thirds of the water present at saturation was released at $\psi \geq -85$ kPa from the control whereas $\psi \geq -150$ kPa is needed to release the same amount of water from all biochar-amended samples. Unexpectedly, soil samples amended with unoxidized biochars (i.e. QS-PW-350, QS-PW-600, QS-PB-350) retained less water at ψ from −0.1 to −5 kPa compared to the control, and contained equivalent amount of water as that of soil control at dry range ($\psi \leq -300$ kPa). However, we observed that oxidized biochar-soil mixtures (e.g. QS-PW-350-A and QS-PB-350-A) held significantly more water than their counterparts except at the saturation region between −0.1 and −5 kPa of ψ. As seen in Table 7, a significant correlation occurred between the total acidic functional groups on biochar surfaces and water contents at different matric potentials indicating the important role of surface functionalities in retaining soil water.

Table 5 summarizes the measured and fitted saturated (θ_s), residual (θ_r) water contents, and the shape parameters (α, n and m) of the van Genuchten (1980) model. The fitted parameters to the SWRCs had coefficients of determination (r^2) close to unit, indicating that the fitting of the proposed interpolation equation to the experimental data was highly acceptable. Application of biochar decreased both the saturated and the residual water contents. Comparable to treatments with unoxidized biochars, the oxidized biochars increased the saturated soil water contents on average by 1.4% and the residual water contents by 0.45%. In addition, treatments with oxidized biochars had lower α values than those with unoxidized biochars.

3.3. Response of soil hydrological variables to biochar porosity and surface chemistry

Table 6 shows the effect of the application of biochar on selected physicochemical and hydrological properties of the sand. The varying pH values in biochars resulted in varying pH values of amended QS soil samples. When we added high pH biochar (i.e. HP-600) to QS soil,

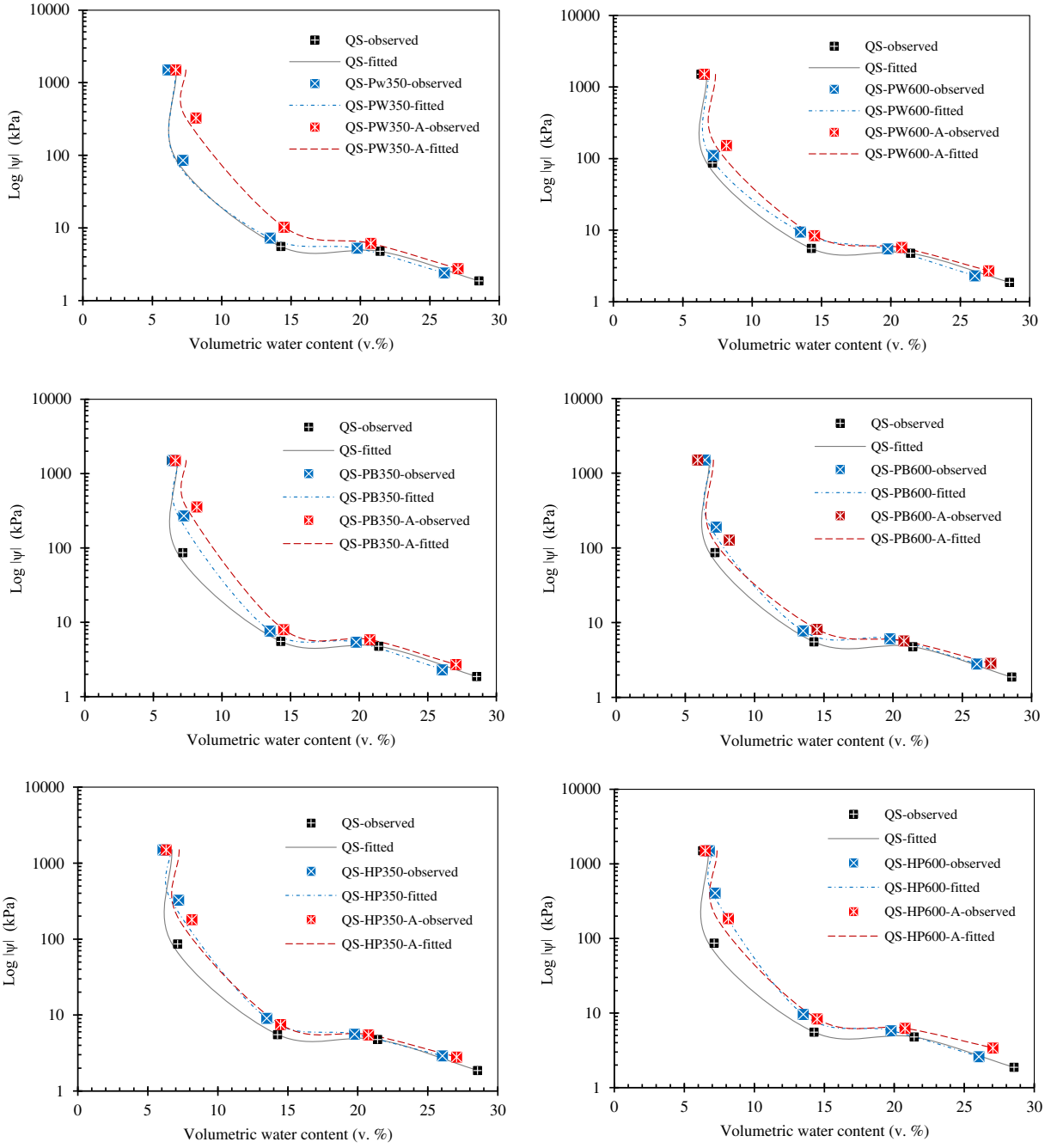

Fig. 4. Predicted soil water retention curves (lines) and measured soil volumetric water contents (symbols) at different matric potentials. Note: Oxidized biochars was abbreviated with letter (A). Estimates of shape parameters are presented in Table 4.

we observed increased pH; the highest values (pH = 9) was found in HP-600 biochar-amended QS soil. Addition of biochar reduced the soil bulk density in all treatments; bulk density in soil samples amended with unoxidized PW-350 and PW-600 biochars, for example, were 0.22 and 0.23 $g \cdot cm^{-3}$ lower, respectively, compared to the control. The biochars have also an impact on soil water content at field capacity (θ_{FC}); the θ_{FC} of QS sand was increased by roughly 8.5% after biochars additions. The θ_{FC} of QS dramatically increased after the addition of oxidized biochars; the highest amount of water retained at field capacity (30.22%) was observed in oxidized HP350-amended samples. This sequence indicated that after oxidation, the biochar surface became less hydrophobic due formation of oxygen complexes which provides sites for surface functionalization.

The majority of the total water potentially stored was available for plant growth in biochar amended QS soil samples compared to the control in which most of this water was easily lost by gravity. The higher available water content (AWC) observed in the oxidized biochar treatments was an important finding. The oxidized HP350-amended sample had the highest AWC, as seen in Fig. 5. Altogether, amended samples show increased water content at the permanent wilting point (PWP) relative to the control. However, water content at PWP presented weak dependencies on the biochar feedstock as well as pyrolysis temperature. The osmotic potential is customarily ignored due to the lack of semipermeable membranes in soil water systems. Here, the osmotic potential was calculated as a function of the EC values of biochars just to get an indication of the potential effects of biochar on this parameter.

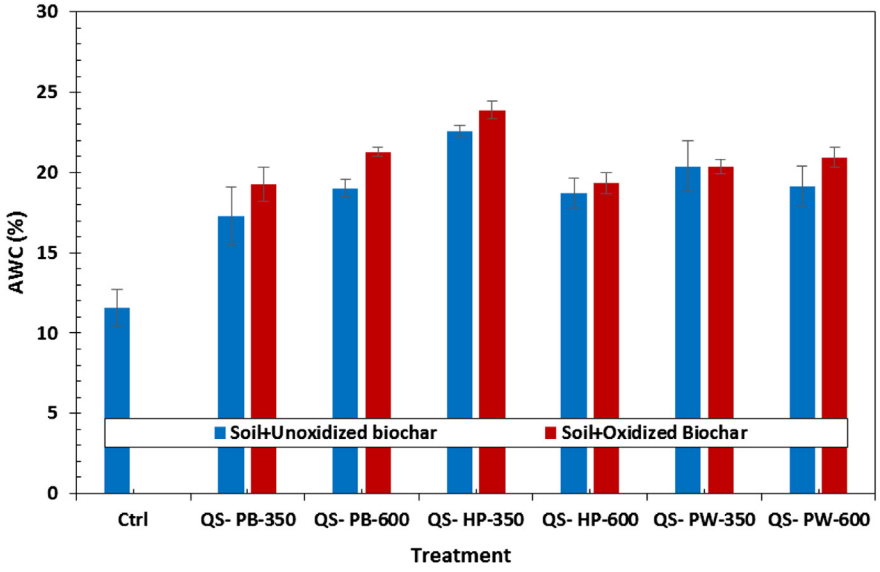

Fig. 5. Effect of biochar on available water capacity (AWC). Error bars show standard deviations and treatment means.

The osmotic potentials appeared highly dependent on production temperature of the biochar, which causes an increase of some inorganic components of biochar.

Our results show that the consistent increase in soil water retention curve (SWRC) is related to an increase in soil moisture at ≤− 30 kPa for treatments with raw (unoxidized) biochars, which in turn could be linked to their physical properties such as porosity (i.e. cavities in micro-range) and surface area. This observation is consistent with a previous theoretical reasoning by Lehmann and Joseph (2009) suggesting that a net increase in water retention results from the high surface area of biochar compared with the low surface area of un-amended sand. Therefore, biochars with enhanced micro-porosity should ideally have higher water retention capability, as demonstrated by Lei and Zhang (2013). This statement confirms findings from other studies that biochar increases soil water retention likely due to the characteristics of its micropores (de Melo Carvalho et al., 2014; Dempster et al., 2012). Dempster et al. (2012), for example, found that volumetric soil moisture content at −100 and −1500 kPa increased significantly when a biochar with 273 $m^2\ g^{-1}$ SA was applied into a sand at 1.8 wt.% application rate. The HP350 biochar we used has approximately

Table 5
Fitted and measured values of the residual water content (θ_r) and the saturated water content (θ_s), and the fitted values of parameters (α, n and m) of the soil water retention model.

		QS-PW-350		QS-PW-600		QS-PB-350		QS-PB-600		QS-HP-350		QS-HP-600	
Parameters	QS	UO	AO	UO	AO	UO	AO	UO	AO	UO	AO	UO	AO
θ_s	28.50[a]	26.06	27.05	26.06	27.06	26.06	27.10	26.06	27.10	26.05	27.06	26.06	27.06
($cm^3\ cm^{-3}$)	28.60[b]	26.38	28.30	27.19	27.75	26.44	27.37	26.15	27.82	28.00	27.00	27.13	27.64
θ_r	6.32[a]	6.15	6.69	6.60	6.60	6.41	6.60	6.41	5.90	6.09	6.32	6.79	6.52
($cm^3\ cm^{-3}$)	6.73[b]	6.68	7.42	6.84	7.36	6.81	7.38	6.81	7.02	6.65	7.24	7.01	7.34
α (cm^{-1})	0.20	0.18	0.16	0.19	0.16	0.17	0.16	0.16	0.15	0.18	0.17	0.17	0.15
n	9.44	4.46	2.85	2.80	3.72	4.17	4.52	5.98	3.86	2.96	4.48	3.03	4.78
m	0.89	0.78	0.65	0.64	0.73	0.76	0.78	0.83	0.74	0.66	0.78	0.67	0.79
r^2	0.999	0.998	0.996	0.996	0.996	0.999	0.996	0.999	0.999	0.998	0.994	0.999	0.999

Abbreviations: θ_s = the saturated water content [$cm^3\ cm^{-3}$] when $\psi \leq -3$ kPa; θ_r = the residual water content [$cm^3\ cm^{-3}$] at $\psi \leq -1500$ kPa; α, n and m = shape parameters of the van Genuchten (1980) model; UO = unoxidized biochar; AO = air-oxidized biochar. van Genuchten parameters were fitted to the data between ≈1.8 and 1500 kPa only. The parameters are therefore only valid for this water potential range.

[a] The measured values of θ_s and θ_r.

[b] The fitted values of θ_s and θ_r.

Table 6
Effect of biochar application to sand on bulk density, pH, EC, water contents at field capacity, plant available water contents and osmotic potentials.

		QS-PW-350		QS-PW-600		QS-PB-350		QS-PB-600		QS-HP-350		QS-HP-600	
Property	QS	UO	AO	UO	AO	UO	AO	UO	AO	UO	AO	UO	AO
Bulk density ($g\ cm^{-3}$)	1.49	1.27	1.28	1.26	1.27	1.28	1.27	1.29	1.27	1.28	1.26	1.27	1.28
pH_{H2O} (1:5)	7.5	8.1	7.8	8.12	7.9	8.1	7.5	8.7	8.2	8.4	8.1	9.0	8.4
EC_{H2O} ($ds\ m^{-1}$)	0.08	0.01	0.01	0.02	0.04	0.02	0.03	0.06	0.06	0.03	0.04	0.06	0.05
θ_{FC} (%)	16.91	26.55	27.09	25.70	27.50	23.68	25.87	25.43	27.18	28.68	30.22	25.50	25.86
θ_{PWP} (%)	5.32	6.15	6.69	6.56	6.56	6.41	6.60	6.41	5.89	6.09	6.32	6.79	6.52
θ_{AWC} (%)	11.59	20.40	20.40	19.15	20.94	17.27	19.27	19.02	21.29	22.59	23.90	18.71	19.34
O_{sm} (−kPa)	2.88	0.36	0.72	0.72	1.44	0.72	1.8	2.16	1.44	1.08	0.36	2.16	0.72

Abbreviations/notes: UO = unoxidized biochar; AO = air-oxidized biochar, WFPS = water filled pore space; θ_{FC} = water content at field capacity; θ_{AWC} = available water content; θ_{PWP} = water content at permanent wilting point (−1.5 MPa); O_{sm} = osmatic potential. Values are averages over the replicates of the treatments (n = 3).

Table 7
Pearson correlations between; soil water retention properties, selected biochar properties and bulk densities of biochar-amended QS soil.

	$\theta_{0\ kPa}$	$\theta_{-10\ kPa}$	$\theta_{-33\ kPa}$	$\theta_{-100\ kPa}$	$\theta_{-500\ kPa}$	$\theta_{-1500\ kPa}$	TC	TAFG	BD
$\theta_{0\ kPa}$	1.00								
$\theta_{-10\ kPa}$	0.25	1.00							
$\theta_{-33\ kPa}$	0.04	0.72**	1.00						
$\theta_{-100\ kPa}$	0.13	0.55**	0.94**	1.00					
$\theta_{-500\ kPa}$	0.04	0.77**	0.80**	0.72**	1.00				
$\theta_{-1500\ kPa}$	0.04	0.73**	0.55**	0.43*	0.82**	1.00			
TC	0.21	0.19	−0.23	−0.36	−0.23	0.09	1.00		
TAFG	0.36*	0.48*	0.51*	0.53*	0.63*	0.28	−0.73**	1.00	
BD	−0.28*	−0.84**	−0.45*	−0.27*	−0.64*	−0.73**	−0.14	−0.46	1.00

0 kPa, −10 kPa, −33 kPa, −100 kPa, −500 kPa, −1500 kPa, water contents at 0, −10, −33, −100, −500, and −1500 kPa matric potentials; TC, total carbon content (wt.%); TAFG, total acidic functional groups on biochar surface; BD, bulk density.
* $P < 0.05$.
** $P < 0.01$.

similar SA to the biochar used by Dempster et al. (2012) and same significant increase in the water content at −100 kPa, but not at −1500 kPa. The conditions of experimental setup are probably the main cause for these discrepancies, regardless of biochar production conditions.

A Pearson's correlation analysis, Table 7, was conducted to identify potential relationships between selected biochar properties and soil water retention characteristics obtained from previous SWRCs. As shown in the table, soil water contents at different matric potentials were significantly inter-correlated ($P < 0.01$) and correlated with bulk densities of biochar-amended soil samples. The bulk density is controlled by the volume occupied by the internal cavities in the biochar. SEM images (Suliman et al., 2016a) demonstrated that all biochars studied contained cavities (large pores) between 0.5 and 300 μm in diameter. These pores could play an important role for increasing soil water retention comparable to soil alone. This postulation is in agreement with (Abel et al., 2013; Carrier et al., 2012; Kinney et al., 2012). Moreover, we could not find any correlations between biochar surface area and pore volume measured by CO_2 adsorption isotherms (Suliman et al., 2016a,b). This was expected because internal porosity measured via CO_2 isotherms fall within a nano-range scale which may not be accessible to the water. In contrast, there was significant correlations observed between total acidic functional groups on biochar surfaces and water contents at different matric potentials. Effects of these surface groups on soil water retention became more significant as matrix potentials decrease from 0 kPa to −500 kPa ($r = 36$ and 63 at 0 kPa and −500 kPa, respectively), indicating their capability for adsorbing and holding water molecules within this range. Furthermore, soil water contents were well-correlated with soil bulk density at −10 kPa and −1500 kPa ($r = -84$ and −73, respectively) after biochar additions, implying that soil water retention at lower matric potentials were mainly affected by biochar cavities (reflected in bulk density measurements) along with surface functionality. Correlation was almost identical in biochars with higher oxygenated functional groups especially in the range of from −10 kPa to −1500 kPa. Our findings are in accordance with those reported elsewhere (Barnes et al., 2014; Yang et al., 2014).

4. Conclusion

In this study we explored the contribution of biochar bulk and surface characteristics on water retention capacity of biochar-Quincy sand blends. The results reported here offer new information regarding the potential of using oxidized biochars to retain more water in sandy soils than the using fresh/raw biochars, demonstrating that post-pyrolysis hot air oxidation could be an effective way to enhance water-holding capacities of biochars. The increase in soil water retention when oxidized biochars were added into the soil can be explained by the increase in the oxygen function groups on the surface of these biochars. However, the better performance of biochar in terms of water retention was actually due to the combination of several properties (i.e. porosity, acidic functional groups) and could not be attributed to only one property of biochar. Our results also suggest that water retention of biochar is controlled by several parameters. The internal porosity of the biochar which influences the bulk density of the biochar, the surface chemistry of the biochar and the source of feedstock that control the hydrophobicity and porosity of the material, along with production temperature.

Acknowledgements

The authors would like to acknowledge the financial support by the Washington State Department of Ecology (C1600095) through the Wastes to Fuel program and by the Washington Department of Agriculture for their support through the Appendix-A program and the Agriculture and Food Research Initiative Competitive grant no. 2011-68005-30416. The authors are also very thankful to the Agricultural Research Center (NIFA-Hatch-WNP00701) and the Washington State Department of Agriculture for the financial support provided.

Appendix A. Supplementary data

Supplementary data to this article can be found online at http://dx.doi.org/10.1016/j.scitotenv.2016.09.025.

References

Abel, S., Peters, A., Trinks, S., Schonsky, H., Facklam, M., Wessolek, G., 2013. Impact of biochar and hydrochar addition on water retention and water repellency of sandy soil. Geoderma 202–203, 183–191. http://dx.doi.org/10.1016/j.geoderma.2013.03.003.
Barnes, R.T., Gallagher, M.E., Masiello, C.A., Liu, Z., Dugan, B., 2014. Biochar-induced changes in soil hydraulic conductivity and dissolved nutrient fluxes constrained by laboratory experiments. PLoS One 9, e108340. http://dx.doi.org/10.1371/journal.pone.0108340.
Basso, A.S., Miguez, F.E., Laird, D.a., Horton, R., Westgate, M., 2013. Assessing potential of biochar for increasing water-holding capacity of sandy soils. GCB Bioenergy 5, 132–143. http://dx.doi.org/10.1111/gcbb.12026.
Bradley, R.H., Smith, M.W., Andreu, A., Falco, M., 2011. Surface studies of novel hydrophobic active carbons. Appl. Surf. Sci. 257, 2912–2919. http://dx.doi.org/10.1016/j.apsusc.2010.10.089.
Carrier, M., Hardie, A.G., Uras, Ü., Görgens, J., Knoetze, J.(.H.)., 2012. Production of char from vacuum pyrolysis of South-African sugar cane bagasse and its characterization as activated carbon and biochar. J. Anal. Appl. Pyrolysis 96, 24–32. http://dx.doi.org/10.1016/j.jaap.2012.02.016.
Copeland, C., Downie, A., Zwieten, L.V., Kimber, S., 2008. The role of a scoping study in directing and supporting the establishment of a slow pyrolysis plant in northern NSW. Australia Wollongbar Agricultural Institute is the Pasture Trial, pp. 1–9.
Das, O., Sarmah, A.K., 2015. The love-hate relationship of pyrolysis bio-char and water: a perspective. Sci. Total Environ. 512–513, 682–685. http://dx.doi.org/10.1016/j.scitotenv.2015.01.061.
de Melo Carvalho, M.T., de Holanda Nunes Maia, A., Madari, B.E., Bastiaans, L., van Oort, P.A.J., Heinemann, A.B., Soler da Silva, M.A., Petter, F.A., Marimon Jr., B.H., Meinke, H., 2014. Biochar increases plant-available water in a sandy loam soil under an aerobic rice crop system. Solid Earth 5, 939–952. http://dx.doi.org/10.5194/se-5-939-2014.
Dempster, D.N., Jones, D.L., Murphy, D.V., 2012. Clay and biochar amendments decreased inorganic but not dissolved organic nitrogen leaching in soil. Soil Res. 50, 216. http://dx.doi.org/10.1071/SR11316.
Forbes, M.S., Raison, R.J., Skjemstad, J.O., 2006. Formation, transformation and transport of black carbon (charcoal) in terrestrial and aquatic ecosystems. Sci. Total Environ. 370, 190–206. http://dx.doi.org/10.1016/j.scitotenv.2006.06.007.

Gray, M., Johnson, M.G., Dragila, M.I., Kleber, M., 2014. Water uptake in biochars: the roles of porosity and hydrophobicity. Biomass Bioenergy 61, 196–205. http://dx.doi.org/10.1016/j.biombioe.2013.12.010.

Kinney, T.J., Masiello, C.a., Dugan, B., Hockaday, W.C., Dean, M.R., Zygourakis, K., Barnes, R.T., 2012. Hydrologic properties of biochars produced at different temperatures. Biomass Bioenergy 41, 34–43. http://dx.doi.org/10.1016/j.biombioe.2012.01.033.

Lehmann, J., Joseph, S., 2009. Biochar for Environmental Management: Science and Technology. first ed. Earthscan, London, UK.

Lehmann, J., Pereira, J., Steiner, C., Nehls, T., Zech, W., Glaser, B., 2003. Nutrient availability and leaching in an archaeological Anthrosol and a Ferralsol of the Central Amazon basin: fertilizer, manure and charcoal amendments, 343–357.

Lehmann, J., Gaunt, J., Rondon, M., 2006. Bio-char sequestration in terrestrial ecosystems — a review. Mitig. Adapt. Strateg. Glob. Chang. 11, 395–419. http://dx.doi.org/10.1007/s11027-005-9006-5.

Lei, O., Zhang, R., 2013. Effects of biochars derived from different feedstocks and pyrolysis temperatures on soil physical and hydraulic properties. J. Soils Sediments 13 (9), 1561–1572.

Liang, B., Lehmann, J., Solomon, D., Kinyangi, J., Grossman, J., O'Neill, B., Skjemstad, J.O., Thies, J., Luizão, F.J., Petersen, J., Neves, E.G., 2006. Black carbon increases cation exchange capacity in soils. Soil Sci. Soc. Am. J. 70, 1719. http://dx.doi.org/10.2136/sssaj2005.0383.

Low, A.P., Stark, J.M., Dudley, L.M., 1997. Effects of soil osmotic potential on nitrification, ammonification, N-assimilation, and nitrous oxide production. Soil Sci. 16–27.

Maia, C., Madari, B., Novotny, E., 2011. Advances in biochar research in Brazil. Dyn. Soil Dyn. Plant 5, 53–58.

Mualem, Y., 1986. Methods of soil analysis: part 1—physical and mineralogical methods. SSSA Book Series. Soil Science Society of America, American Society of Agronomy, Madison http://dx.doi.org/10.2136/sssabookser5.1.2ed.c31.

Novak, J.M., Busscher, W.J., Laird, D.L., Ahmedna, M., Watts, D.W., Niandou, M.a.S., 2009a. Impact of biochar amendment on fertility of a southeastern coastal plain soil. Soil Sci. 174, 105–112. http://dx.doi.org/10.1097/SS.0b013e3181981d9a.

Novak, J., Lima, I., Xing, B., Gaskin, J., Steiner, C., Das, K., Ahmedna, M., Rehrah, D., Watts, D., Busscher, W., Schomberg, H., 2009b. Characterization of designer biochar produced at different temperatures and their effects on a loamy sand. Ann. Environ. Sci.

Quin, P.R., Cowie, A.L., Flavel, R.J., Keen, B.P., Macdonald, L.M., Morris, S.G., Singh, B.P., Young, I.M., Van Zwieten, L., 2014. Oil mallee biochar improves soil structural properties—a study with X-ray micro-CT. Agric. Ecosyst. Environ. 191, 142–149. http://dx.doi.org/10.1016/j.agee.2014.03.022.

Rossi, C., Nimmo, J.R., 1994. Modeling of soil water retention from saturation to oven dryness. Water Resour. Res. 30, 701–708.

Seki, K., 2007. SWRC fit — a nonlinear fitting program with a water retention curve for soils having unimodal and bimodal pore structure. Hydrol. Earth Syst. Sci. Discuss. 4, 407–437. http://dx.doi.org/10.5194/hessd-4-407-2007.

Sika, M.P., 2012. Effect of biochar on chemistry, nutrient uptake and fertilizer mobility in sandy soil.

Song, W., Guo, M., 2012. Quality variations of poultry litter biochar generated at different pyrolysis temperatures. J. Anal. Appl. Pyrolysis 94, 138–145. http://dx.doi.org/10.1016/j.jaap.2011.11.018.

Stoof, C.R., Wesseling, J.G., Ritsema, C.J., 2010. Effects of fire and ash on soil water retention. Geoderma 159, 276–285. http://dx.doi.org/10.1016/j.geoderma.2010.08.002.

Suliman, W., Harsh, J.B., Abu-Lail, N.I., Fortuna, A.-M., Dallmeyer, I., Garcia-Perez, M., 2016a. Influence of feedstock source and pyrolysis temperature on biochar bulk and surface properties. Biomass Bioenergy 84, 37–48. http://dx.doi.org/10.1016/j.biombioe.2015.11.010.

Suliman, W., Harsh, J.B., Abu-Lail, N.I., Fortuna, A.-M., Dallmeyer, I., Garcia-Perez, M., 2016b. Modification of biochar surface by air oxidation: role of pyrolysis temperature. Biomass Bioenergy 85, 1–11. http://dx.doi.org/10.1016/j.biombioe.2015.11.030.

Uzoma, K.C., Inoue, M., Andry, H., Fujimaki, H., Zahoor, A., Nishihara, E., 2011. Effect of cow manure biochar on maize productivity under sandy soil condition. Soil Use Manag. 27, 205–212. http://dx.doi.org/10.1111/j.1475-2743.2011.00340.x.

van Genuchten, M.T., 1980. Closed-form equation for predicting the hydraulic conductivity of unsaturated soils. Soil Sci. Soc. Am. J. 44, 892–898.

Verheijen, F.G., Jeffery, S., Bastos, A.C., van der Velde, M., Diafas, I., 2010. Biochar application to soils. EUR 24099 EN. Office for the Official Publications of the European Communities, Luxembourg http://dx.doi.org/10.2788/472.

Yang, F., Zhang, G.-L., Yang, J.-L., Li, D.-C., Zhao, Y.-G., Liu, F., Yang, R.-M., Yang, F., 2014. Organic matter controls of soil water retention in an alpine grassland and its significance for hydrological processes. J. Hydrol. 519, 3086–3093. http://dx.doi.org/10.1016/j.jhydrol.2014.10.054.